Combined study of radiation belts by the satellite particle telescope STEP-F and solar soft X-ray photometer SphinX during recent deep minimum of solar activity

O. V. Dudnik, Institute of Radio Astronomy, National Academy of Sciences of Ukraine (IRA NASU); V. N. Karazin Kharkiv National University, Kharkiv, Ukraine, dudnik @rian.kharkov.ua
P. Podgórski, Solar Physics Division, Space Research Centre, Polish Academy of Sciences (SPD SRC PAS), Wroclaw, Poland, pp @cbk.pan.wroc.pl
J. Sylwester, Solar Physics Division, Space Research Centre, Polish Academy of Sciences (SPD SRC PAS), Wroclaw, Poland, js @cbk.pan.wroc.pl

Abstract
We present new features detected in the high energy particle distributions of the Earth's magnetosphere during deep minimum of the solar activity. They came as a result of data analysis derived from the STEP-F and SphinX devices. Both instruments have flown in 2009 onboard the *CORONAS-Photon* satellite. Due to orthogonal orientation of viewing axes of STEP-F and SphinX we have seized an opportunity to study anisotropy of particle fluxes in different volumes of the near Earth space at the height of ~ 550 km.
Data analyses revealed that Sun-oriented soft X-ray photometer SphinX detected electrons of intermediate and subrelativistic energies and their bremsstrahlung emission in the highest two channels of 8-bit energy spectra. Hence, the SphinX extended energy range of particle registered by STEP-F towards lower energies.
In the research presented three-belt's configuration of enlarged electron fluxes in the magnetosphere, directivity of particle velocities, variability of energy spectra in different zones of magnetosphere are discussed. We consider electron flux pulsations during various phases of geomagnetic activity as an important constituent of space weather.
Keywords: magnetosphere, space, radiation belt, electrons, energy spectrum, anisotropy

1. INTRODUCTION

The satellite telescope of electrons and protons STEP-F was constructed to study spatial and temporal distributions of high energy particles in the Earth's magnetosphere (Dudnik et al., 2011). The SphinX solar spectrophotometer in X-rays also was a part of the complex of scientific apparatus of the *CORONAS−Photon* low Earth orbit satellite (Sylwester et al., 2008; Gburek et al., 2011). During processing of the data derived from this instrument it was found out that counting rates in channels of analog-to-digital converter (ADC), corresponding to highest energy photons, are substantial even during spacecraft passages over the night intervals of the orbit. The counting rates in these channels increased sharply with the satellite passage of regions of the South Atlantic Anomaly (SAA) and radiation belts suggesting the response of SphinX detectors to presence of ambient high energy particles (Podgórski et al., 2012).

Detector unit STEP–FD of the STEP–F instrument was located in close proximity to the SphinX. This enabled us to perform joint analysis of the data obtained from the particle detection channels of the SphinX X-ray spectrophotometer and STEP–F channels recording electrons and protons of different energy ranges. In this work we analyze spatial and temporal distributions of the electron fluxes inside and outside the Van Allen electron radiation belts observed in May 2009, during the deep minimum of 11-year's cycle of the solar activity based on the data obtained from the STEP-F and the SphinX devices onboard the low Earth near polar circular orbit *CORONAS-Photon* satellite as a constituent of payload science package (Figure 1).

Figure 1. Overall view of the payload of low Earth circular near polar orbit CORONAS-Photon satellite. Credit of the Moscow Engineering Physics Institute.

2. DETECTION OF THREE-BELT'S CONFIGURATION OF ENHANCED PARTICLE FLUXES IN THE EARTH'S MAGNETOSPHERE

2.1. Space weather indices in May 2009

Some parameters of geophysical conditions in the near Earth space are presented in Figure 2.

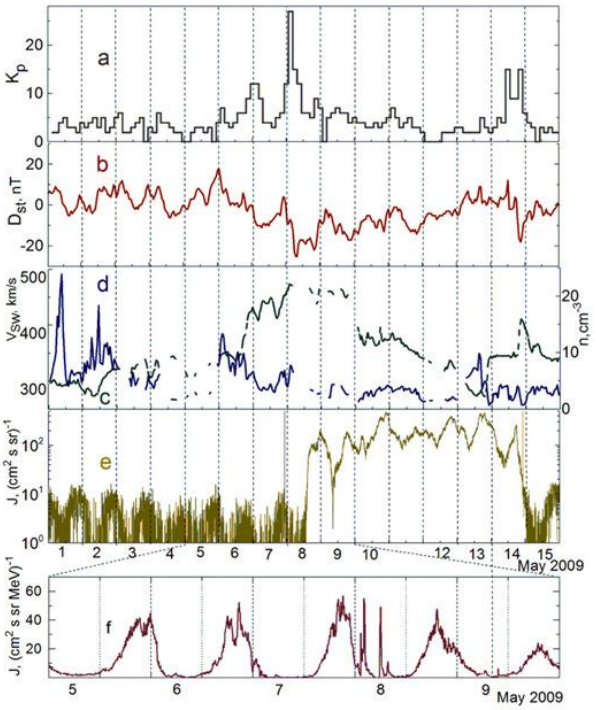

Figure 2. Parameters of geomagnetic field, solar wind and particle fluxes at geostationary orbit at 1st half of May 2009.

Shown are geomagnetic K_p- (a) and D_{st}-indices (b), solar wind velocity V_{sw} (c) and density n (d) as measured by CELIAS/MTOF/PM proton monitor onboard the *SOHO* spacecraft situated at the L1 Lagrangian point on the Earth – Sun line. Figure 2 shows also electron fluxes with energies $E_e > 2$ MeV (e) and protons of $E_p = 0.8 – 4.0$ MeV (f) as observed by GOES-11 geostationary satellite. It is seen that within the period from 6 to 14 May, a weak storm ($D_{st} \approx$ - 30 nT) took place with the main phase on May, 8 from ~ 06 : 00 to ~ 09 : 00 UT. The initial phase took place from ~ 06 : 00 to ~ 09 : 00 observed at the beginning of May 6. Just after growth of solar wind density STEP-F detected enhanced electron fluxes in the Van Allen radiation belts (Figure 3, yellow and crimson curves).

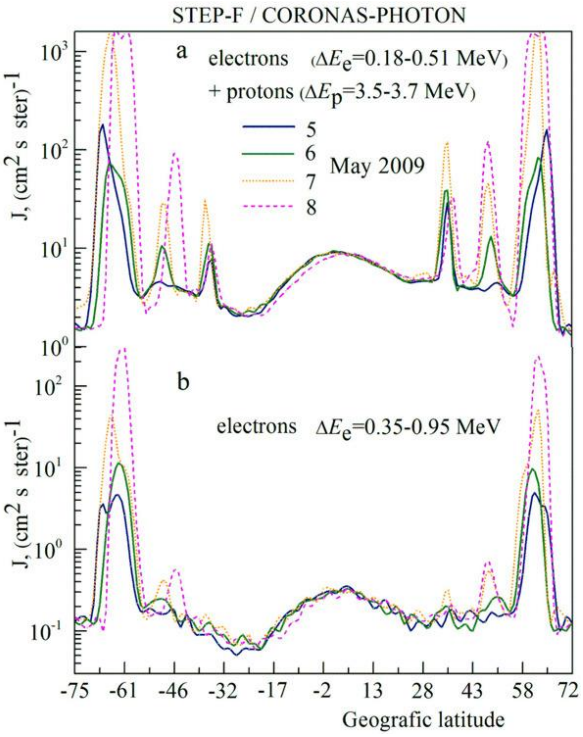

Figure 3. Fluence of particle intensity over the period of 5 - 8 May, 2009. Different colors/lines represent individual days as indicated.

2.2. Additional inner electron radiation belt

Figure 3 demonstrates particle flux variations in two energy ranges. Observations represent data with 30-seconds's resolution collected on every 9th ascending nodes of satellite orbit covering latitude range from - 75^0 north to + 72^0 south over period from May 5 to May 8, 2009. Satellite crossing of classical outer and inner radiation belts is clearly seen in Southern and in Northern hemispheres. Figure 3 reveals presence of the third, additional to a pair of classical belts of the Earth's magnetosphere being crossed by the satellite at - 35 ÷ - 32 degrees south, and at ~ 36 ÷ 42 degrees north. Accordingly, these latitudes correspond to McIlwain parameter $L \approx 1.6$.

Cross-analysis of Figures 2 and 3 indicates that the main phase of substorm is associated with a sharp and substantial (more than one order of magnitude) increase

of electron fluxes below the outer belt in two energy ranges of STEP-F, accompanied by considerable enhancement of two-MeV's electron fluxes at geostationary orbit as observed by GOES-11.

In the first publication about additional inner radiation belt derived from the STEP-F data (Dudnik, 2010) it was stated that 2 inner radiation belts: on $L \approx 2.28$, and on $L \approx 1.61$ were detected in the energy range $\Delta E_e = 0.18 \div 0.51$ MeV (D1e energy channel). Persistent presence of the third belt on lower L-shell, and the time variation of electron population in both belts are observed depending on the overall level of geomagnetic activity. All belts are clearly seen at geographical longitudes that do not coincide with SAA's longitudes (Dudnik et al., 2012; Dudnik, 2012).

2.3. Mapping at the altitude of ~ 550 km in terms of electron fluxes on the range $E_e = 0.18 \div 0.51$ MeV.

The satellite orbit has crossed all longitudes between $\pm 82^0$ 15 times during 24h period. This allowed us to construct daily maps of the particle content in terms of high energy electron fluxes at the height of ~ 550 km. Results are shown in Figure 4 for the electrons of energy range $\Delta E_e = 0.18 \div 0.51$ MeV on May 8, 2009 in selected color scales of particle flux densities. Figure 4a represents map of flux density of ~ 1500 particles / (cm^2 × s × ster) marked by red color, while Figure 4b represents regions with minimum fluxes where maximal flux density of ~ 15 particles / (cm^2 × s × ster) is marked also in red.

3. SPHINX X-RAY SPECTROPHOTOMETER AS DETECTOR OF CHARGE PARTICLES

3.1. Sensitivity of SphinX to energetic particles

Detectors of SphinX were not initially dedicated to observations of the particle content. Their reactions to presence of particles were unknown before the launch. In order to find the sensitivity of silicon large area photodiodes Det1 and Det2 of the SphinX to a presence of ambient energetic particles we have performed comparison of obtained data with well-calibrated STEP-F recordings during the geomagnetic substorm on May 8, 2009 (Podgórski et al., 2012). Detectors Det1 and Det2 were equipped with the front-end collimators limiting the field of view to a very narrow cone centered on the Sun. These collimators operated in the soft X-ray domain and for particles of sufficiently low energy. However, for high-energy gamma quanta and secondary emission arising from primary electron's interaction with the detector head materials, entire TESIS instrument, and the satellite itself the emission can be observed from particle coming from larger solid angles. As a consequence Det1 and Det2 detectors of SphinX are sensitive to a mixture of electron ambient populations namely to electrons and the secondary γ–quanta, generated by magnetospheric high energy electrons. The latter allowed us to introduce the concept of effective lower energy thresholds for electron detection (E_{thr1} and E_{thr2}) by Det1 and Det2 detectors, respectively.

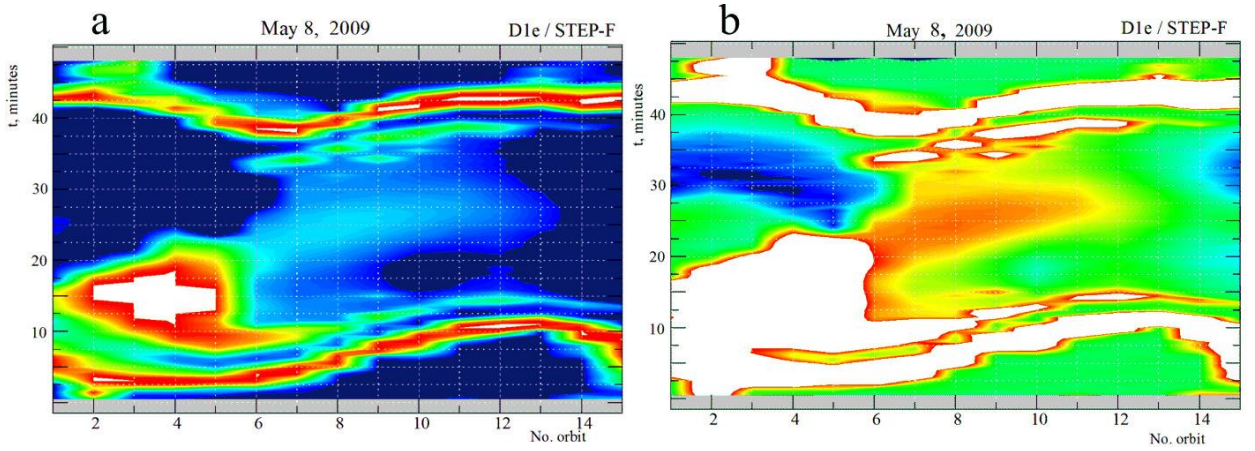

Figure 4. The map in terms of electron flux density of energies 0.18 ÷ 0.51 MeV on the height of ~ 550 km during the main phase of geomagnetic substorm of May 8, 2009. Y axis corresponds to time phase of the semi-circle on the ascending part of satellite orbit counted from the maximum latitude in the Southern hemisphere.

Clearly seen are global zones of enhanced particle fluxes in the SAA, in Van Allen outer and inner radiation belts in both hemispheres, the third radiation belts (from ~ 7th to ~ 11th orbit of the day. Specific feature on the map is persistent presence of the enlarged electron fluxes from the SAA zone to the volume of low and near-equatorial latitudes toward the eastern longitudes.

3.2 Effective lower energy thresholds of electrons detected by SphinX's sensors in SAA

The analysis of averaged over 14 days of May, 2009 L-shell values with maximum particle intensities vs. electron energy allowed us to determine values of effective lower threshold energies E_{thr1} and E_{thr2}. We determined also the lower threshold effective energy of

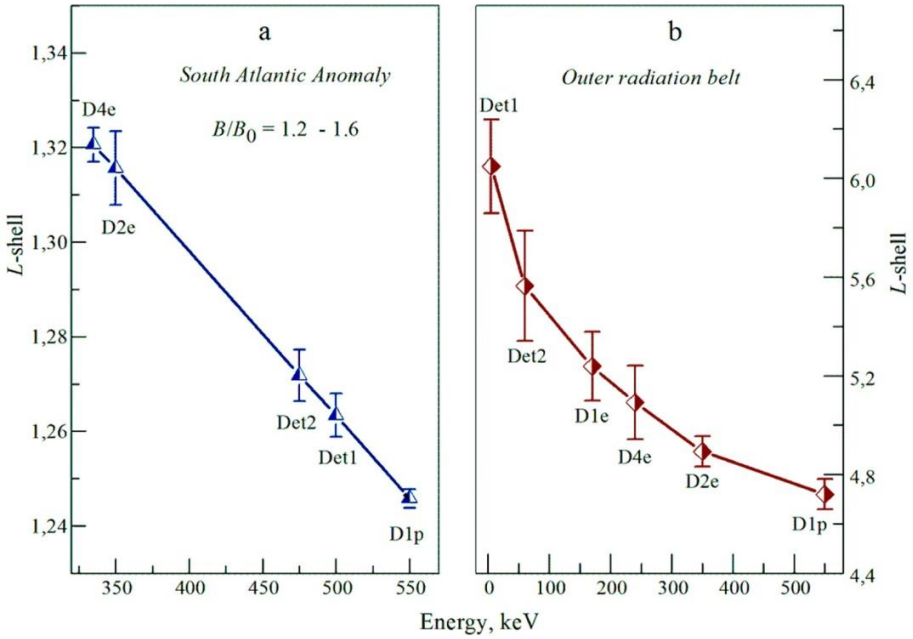

Figure 5. a - Dependence of averaged L-shell values corresponding to maximum electron flux densities on the particle energy recorded in the SAA, b – dependence of averaged L-shell values on the particle energy corresponding to highest electron fluxes measured in outer belt of Northern hemisphere.

STEP-F's D4e channel, where D4 is fourth in telescopic system, i.e. the scintillation CsI(Tl) detector. In Figure 5a we present dependence of *L*–shells with largest particle fluxes, on the electron energy. As a basic point the energies of D2e (electrons with energies E_e = 0.35 ÷ 0.95 MeV) and D1p (electrons with energies E_e = 0.55 ÷ 0.95 MeV + protons with energies E_p = 3.7 ÷ 7.4 MeV) energy channels of STEP-F were chosen.

It can be seen that values of E_{thr1} and E_{thr2} are very close, assuming values ~ 500 keV and ~ 475 keV for Det1 and Det2, respectively. Large dispersion of these values is determined by a poor statistics (14 days analyzed), from one side, and by the diurnal displacement of the satellite position on the longitude at fixed latitude relative to the initial day.

Effective bottom threshold energy of STEP-F's D4e channel was determined from Figure 5a as well: $E_{D4e} \approx 335$ keV. E_{D4e} values varied from day to day in the energy range from 230 to 350 keV during the period of May, 1 – 14, 2009, probably due to variation of electron energy spectrum slope. At the same time all values of E_{D4e} are lower as compared with respective E_{thr1} and E_{thr2} of the SphinX's Det1 and Det2 sensors because of high efficiency of registration by CsI(Tl) scintillation detector resulting from its large active area, and from low electronic noises of the photomultiplier.

3.3. Parametrization of E_{thr1}, E_{thr2}, and E_{D4e} values as applied to the outer radiation belt.

In order to estimate E_{thr1}, E_{thr2}, and E_{D4e} values outside the SAA we have studied the dependence of averaged values of *L*–shells with highest particle flux densities in the Van Allen outer belt on the electron energy. Method is based on the condition that the higher particle energy is, the lower is corresponding *L*-shell in the magnetosphere at which particles drift to on their way from one mirror point in Northern polar oval to the conjugate mirror point in the Southern hemisphere (Horne et al., 2003; Lyons et al., 1972; Lyons, 1974).

Results presented in Figure 5b are obtained for the ninth ascending node of the day orbits in the Northern hemisphere. Noticeable variation of derived electron flux peak position along the *L* – parameter in the outer belt is explained by Δ*L* – displacement of the particle flux peak toward the region of smaller *L*-shells due to obvious influence of geomagnetic substorm which occurred in the analyzed period.

The following values of lower effective threshold energies $E_{thr1} \approx 5$ keV, $E_{thr2} \approx 60$ keV, and $E_{D4e} \approx 240$ keV were defined. Det2 sensor of SphinX was covered by the tantalum plate with the thickness of 400 μm. This means that electrons with energies < 1.2 MeV could not cross through and be detected. However, tantalum plate could serve as a good target for the generation of low energy secondary gamma quanta as a result of its bombardment by high energy magnetospheric electrons.

E_{thr2} value as connected with the outer radiation belt is smaller by a factor fo ~ 10 as compared with that corresponding to SAA region. This comes as a result of the softer character of electron spectrum in the radiation belt. E_{thr2} value is reduced also since a small part of the low energy electron fluxes enters detector window directly through the opening of the area of 4.9×10^{-3}

cm^2, being subsequently recorded by depletion layer of the photodiode.

E_{D4e} values of STEP-F's D4e energy channel corresponding to SAA and the outer radiation belt do not differ significantly from each other because of coincidence logic applied for this channel. Registration of events in D4e is carried out only when associated events are detected simultaneously in all four layers of telescopic system. At the same time decrease of E_{D4e} value from ~ 335 keV in SAA to ~240 keV in outer belt also comes as a result of softening of the energy spectrum in the\is belt.

4. ANISOTROPIC NATURE OF ELECTRON PROPAGATION IN THE BOTTOM LAYERS OF MAGNETOSPHERE

In order to explore spatial distribution of electron velocities we have studied evolution of particle flux densities for the period of May, 1 ÷ 14, 2009 on descending parts 13th orbit of the day. The patterns have been considered for D1e and D2e energy channels of STEP-F, and for the Det1 and Det2 sensors of SphinX instrument. Results are shown in Figure 6. The satellite crossed the outer radiation belt in the Southern hemisphere at latitudes ≈ - 80 ÷ - 72 degrees south, and in the Northern hemisphere at latitudes ≈ 50 ÷ 62 degrees north (zone *1*); inner radiation belt at latitudes - 62 ÷ -50 degrees south, and at ≈ 50 ÷ 62 degrees north (zone *2*); and the peripheral region of the SAA - 35 ÷ - 8 degrees south (zone *3*).

Figure 6 demonstrates almost identical electron fluxes in the outer radiation belt in both hemispheres as measured by STEP-F's D1e and D2e channels. At the same time SphinX did not detected any substantial particle fluxes during the satellite crossing of both classical radiation belts in the Northern hemisphere (bottom parts of the two right-hand patterns). However, Det1 sensor observed substantially enhanced count rates in radiation belts of Southern hemisphere. The effect is also present in Det2 sensor of the SphinX but to a smaller extent.

Having in mind the narrow field of view (~ 2^0 - 3^0) of Det1 and Det2 sensors in SphinX due to presence of collimators, such tangible difference in responses on satellite crossing of the selfsame radiation belt in different hemispheres can be explained by presence of a strong directivity in distribution of particle velocities

Essential distinction in counting rates derived from the SphinX's Det1 and Det2 sensors in Southern and Northern hemispheres does not corresponds to almost identical count rates in both hemispheres as seen in D1e and D2e STEP-F's energy channels. This fact can be explained by different angles of view of both instruments. SphinX was able to discern a directivity

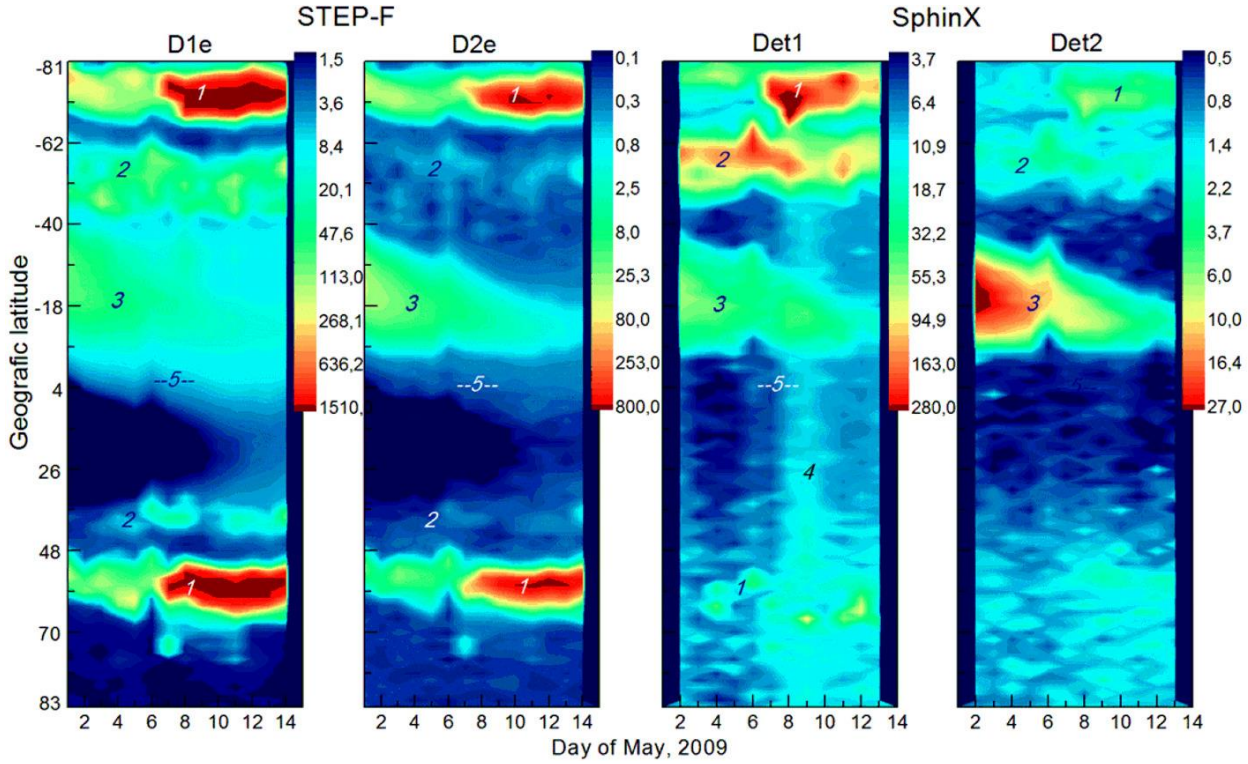

Figure 6. Patterns of particle flux variations during period of May, 1 ÷ 14, 2009 derived from D1e and D2e energy channels of the STEP-F, and from Det1 and Det2 sensors of the SphinX. Specific regions on the plots are: 1: outer radiation belt; 2: inner radiation belt; 3: peripheral region of the SAA; 4: particles recorded by Det1 sensor of the SphinX during the main phase of geomagnetic substorm; 5: geographic equator.

tendency of particle velocities during the mapping of Southern and Northern hemispheres because of small solid angle of view in comparison with a viewing angle in STEP-F. Hence, we suggest that electrons filling radiation belts possess preferential directions of the motion at the heights of the spacecraft orbit.

X-ray spectrophotometer's sensors in the last two ADC channels of dynamic energy spectra have recorded preferably the secondary γ−radiation. γ−quanta energy spectra steeply falling off with increasing energy. Taking into account that response of D1 silicon matrix detector of the STEP-F device had not unnoticeable level to the spacecraft crossing of the inner electron belt at the Southern hemisphere it can be concluded that SphinX's Det1 photodiode confidently observed internal bremsstrahlung emission generated by magnetospheric electrons of energies with upper limit defined by the STEP-F's D1e lower threshold energy, i.e. E_e < 180 keV. This conclusion is additionally confirmed by records of Det1 sensor which revealed precipitating electrons during the main phase of weak geomagnetic substorm of May 8, 2009 in the wide range of latitudes (zone *4*) including the geographic equator (zone *5*).

5. CONCLUSIONS

High sensitivity of STEP-F's detectors to presence of negligible particle fluences allowed us to reveal the existence of additional, third persistent inner electron radiation belt. *L*-profile of this belt with the maximum intensity of electrons being observed at $L_{max} \approx 1.6$, resembles *L*-profiles of classical Van Allen belts. *L*-profile of this new inner belt also does not represent intermittent-type event. We did not detected electrons with energies $E_e \geq 0.4$ MeV in the new "additional" electron radiation belt.

In order to characterize the sensitivity of two X-ray detectors in the SphinX spectrophotometer constructed on the base of silicon PIN large area photodiodes to the presence of ambient energetic particles we have introduced the concept of effective lower energy thresholds of electron registration E_{thr1} for Det1, and E_{thr2} for Det2 sensors of SphinX. We defined corresponding values for these parameters, and found out that pairs of E_{thr1} and E_{thr2} as applied to the SAA, and as applied to outer radiation belt significantly differ from each other. We assume that this difference comes as a result of differences in the energy spectra of electrons filling above referred various regions. It is pointed out that SphinX measurements have substantially expanded and complemented the total energy range of the STEP-F measurements of particle energy spectra.

Finally, comparison and interpretation of data from STEP-F and SphinX instruments for fourteen days in May 2009 allowed us to present evidence for anisotropic character of electron's velocities distribution populating the bottom layers of the Earth's magnetosphere outside the SAA region.

Acknowledgment

Authors acknowledge the support from research project IRA NASU - SRC PAS in the frame of "Agreement on scientific cooperation between the Polish Academy of Sciences and the National Academy of Sciences of Ukraine".

REFERENCES

Dudnik, O., Sylwester, J., Podgórsi, P., Gburek, S., 2012. Radiation belts of the Earth: overview, methods of investigations, recent observations on the CORONAS-Photon spacecraft. *In:* Abstract book of Conference "Progress on EUV&X-ray spectroscopy and imaging", Wroclaw, Poland, November 20-22, 2012, 3.

Dudnik, O., 2012. Unexpected behavior of subrelativistic electron fluxes under Earth radiation belts. *In:* Abstract book of 4th International workshop HEPPA/SOLARIS-2012, Boulder, Colorado, USA, October 9-12, 2012, 15.

Dudnik, A. V., Persikov, V. K., Zalyubovsky, I. I., Timakova, T. G., Kurbatov, E. V., Kotov, Yu. D., Yurov, V. N., 2011. High sensitivity STEP-F spectrometer–telescope for high-energy particles of the CORONAS-PHOTON satellite experiment. *Solar System Research*, **45**, 3, 212–220, doi:10.1134/S0038094611020043.

Dudnik, O. V. 2010. Investigation of the Earth's radiation belts in May 2009 at the low orbit satellite with the STEP-F instrument (in Russian). *Space Science and Technology (Kosmichna Nauka i Tekhnolohiia)*, **16**(5), 12-28.

Gburek, S., Sylwester, J., Kowaliński, M., Bąkala, J., Kordylewski, Z., Podgórski, P., Plocieniak, S., Siarkowski, M., Sylwester, B., Trzebiński, W., Kuzin, S. V., Pertsov, A. A., Kotov, Yu. D., Farnik, F., Reale, F., Philips, K. J. H., 2011. SphinX soft X-ray spectrophotometer: science objectives, design and performance. *Solar System Research*, **45**, 3, 189–199, doi: 10.1134/S0038094611020067.

Horne, R. B., Meredith, N. P., Thorne, R. M., Heynderickx, D., Iles, R, H. A, Anderson, R. R., 2003. Evolution of energetic electron pitch angle distributions during storm time electron acceleration to megaelectronvolt energies. *J. Geophys. Res.*, **108,** A1, 1016, SMP 11-1- SMP 11-13, doi:10.1029/2001JA009165.

Lyons, L. R., Thorne, R. M., Kennel, C. F., 1972. Pitch-angle diffusion of radiation belt electrons within the plasmasphere. *J. Geophys. Res.*, **77**, 3455–3474, doi:10.1029/JA077i019p03455.

Lyons, L. R., 1974. Pitch angle and energy diffusion coefficients from resonant interactions with ion-cyclotron and whistler waves, *J. Plasma Phys.*, **12**(3), 417-432, doi:10.1017/S002237780002537X.

Podgórski, P., Dudnik, O. V., Sylwester, J., Gburek, S., Kowałiński, M., Siarkowski, M., Plocieniak, S., Bąkala, J., 2012. Joint analysis of SphinX and STEP-F instruments data on magnetospheric electron flux dynamics at low Earth orbit. *In*: Abstracts of 39th Scientific Assembly of COSPAR, July 14-22, 2012, Mysore, India. Panel PSW.3: "Space Weather Data: Observations and Exploitation for Research and Applications", STW-C-119 PSW.3-0028-12, 112.

Sylwester, J., Kuzin, S., Kotov, Yu. D., Farnik, F., Reale, F., 2008. SphinX: A fast solar Photometer in X-rays, *J. Astrophys. Astron.*, 29(1-2), 339-343, doi:10.1007/s12036-008-0044-8.

.